Front. Chem. China (2006) 2: 130–137
DOI 10.1007/s 11458-006-0002-4

RESEARCH ARTICLE

Yang Guizhong, Wang Min, Liu Tianxi

The photophysical properties and morphology of fluorene-alt-benzene based conjugated polymer

Abstract A series of fluorene-*alt*-benzene based conjugated main chain polymers chemically attached with alkyl side chains of different lengths on phenylene rings were designed and synthesized by a palladium catalyzed Suzuki coupling reaction. The UV-vis absorption and fluorescence spectra, thermal stability of spectral property, phase transition behavior and morphology of the synthesized polymers were investigated. With increasing the length of the alkyl side chain, the UV and fluorescence spectra exhibit an obvious blue shift compared with those of the unsubstituted polymer. The alkyl substitution improves the thermal spectral stability of the polymers due to the steric hindrance of the alkyl side chains, thus leading to efficient separation of the main chain backbones. The phase transition behavior is closely related to the length of the alkyl side chains attached on the phenylene rings. The annealed films of the polymers display characteristic nematic liquid crystalline texture. TEM observations indicate that solvent-cast thin deposits of all the polymers show typical fibrillar morphology.

Keywords conjugated polymers, optical properties, liquid crystal phase transition, morphology

1 Introduction

There has been wide interest in the photophysical properties of rod-like conjugated polymers because of their potential applications in various optoelectronic devices, especially in polymers light-emitting diodes (PLEDs). Polyfluorenes (PFs)[1–3], polythiophenes (PTs) [4], poly(*p*-phenylenes) (PPPs)[5], poly(*p*-phenylenenvinylenes) (PPVs)[6], and their derivatives are several classes of prime rod-like polymers such as light-emitting materials, due to high quantum efficiencies and excellent prospects for device applications. In general, rigid-rod polymers do not melt and have poor solubility in most organic solvents. Therefore, flexible side chains such as alkyl or alkoxy are always introduced into the rigid-rod polymers to improve their solubility and film-forming characteristics. In addition, side chain substitution is used to confer new functionality and to alter the intramolecular and intermolecular structures at nanometer length scales [7–9]. PFs[10–13], PTs[14], and PPPs [5] substituted with alkyl groups have been heavily studied in the past decade. It has been well documented that the physical properties are significantly affected even by slight changes of the nature of the side chains (e.g. length, branching and organization), the backbone structure, intramolecular and intermolecular packing. The bulky side chain constituents will reduce close packing of the conjugated polymer backbones and thereby diminish the formation of excimers and/or exciplexes[15]. These side chains can also give rise to a rich array and display liquid crystal polymer phases[16–18]. However, the relationship between the side chain moiety and the observed physical properties remains poorly understood. Most models presented so far generally pertain to single polymer chains in an idealized setting[5,19], and the rendering attempts to establish a correlation between morphology and photophysical properties remain rather imprecise. Therefore, systematic investigations regarding photophysical properties and morphology of the polymers with different side chains are clearly needed.

In this study, a series of fluorene-*alt*-benzene based conjugated main chain polymers chemically attached with alkyl side chains of different lengths onto a phenylene ring were designed and successfully synthesized. The spectra in solution and in film, thermal spectral stability, phase transition behavior and morphology of the synthesized polymers were investigated. The effect of alkyl chain length

Yang Guizhong(✉),Liu Tianxi(✉)
The Key Laboratory of Molecular Engineering of Polymers of Chinese Ministry of Education,
Department of Macromolecular Science, Laboratory of Advanced Materials, Fudan University, 220 Handan Road, Shanghai 200433, China.
E-mail: 041055024@fudan.edu.cn; txliu@fudan.edu.cn

on the photophysical property, phase transition behavior and morphology structure of the polymers were studied.

2 Experimental

2.1 Instrumentation

^{1}H and ^{13}C NMR spectra were recorded on Varian Mercury Plus 400 spectrometer in deuterated chloroform solution at ambient temperature with tetramethylsilane as the internal standard. Elemental analyses were carried out on a Vario EL Ⅲ CHNOS Elemental analyzer. Number-average (*Mn*) and weight-average (*Mw*) molecular weights were determined by gel permeation chromatography (GPC) with a HP1100 HPLC system equipped with 7911GP-502 and GP NXC columns. The calibration was made with a series of monodispersed polystyrene standards in THF. UV-visible absorption spectra were recorded on Shimadzu 3150 PC spectrophotometer. Fluorescence measurement was carried out on Shimadzu RF-5301 PC spectrofluorometer with a xenon lamp as a light source. Thermogravimetric analysis (TGA) was conducted on Shimadzu DTG-60H under a heating rate of 10℃/min in nitrogen gas. Differential scanning calorimetry (DSC) was performed on Shimadzu DSC-60A at a heating and cooling rate of 10℃/min and under a stream of nitrogen gas. Polarized light microscopy (PLM) images were recorded on LEICA DM LM/P 11888500 polarized light microscope. The thin films for transmission electron microscopy (TEM) observation were prepared by dropping the dilute solutions (1%-w/v in xylene) onto carbon-coated copper grids. Extra solution was blotted with filter paper. After solvent evaporation, the copolymer films were directly observed using Philips CM300-FEG TEM under an accelerated voltage of 150 kV without staining.

2.2 Materials

Fluorene and 1,4-dibromobenzene were obtained from Aldrich Chemical Co. and used without further purification. 9,9-dihexylfluorene (1)[20], 2,7-dibromo-9, 9-dihexylf luorene (2)[20], 1,4-dialkylbenzene (4)[21] and 1,4-dibromo-2.5-dialkylbenzene [21] were prepared according to the procedures described in the literature.

2.3 Synthesis of 9,9-dihexylfluorene-2,7-bis(trimethylene boronate).

n-Butyllithium (7.6 mL, 12.18 mmol, 1.6 M in hexane) was added dropwise to a solution of (2) (2 g, 4.06 mmol) in THF (30 mL) at –78°C. The mixture was stirred at –78°C for 1 h, and 40.6 mmol of trimethyl borate was added rapidly to the mixture. The solution was stirred at –78°C for another 1 h, then warmed to room temperature and stirred for 20 h. Superfluous HCl (2M) was added to the solution and stirred for 1 h. The mixture solution was extracted with ether, and the organic solvents were removed by extraction under reduced pressure at 30°C to obtain a white solid (diboronic acid). The solid was dissolved in 40 ml toluene, and the solution was refluxed with 1,3-propanediol (0.3 ml) for 10 h. After the usual workup, the crude product was recrystallized from hexane to obtain a white crystal (1.5 g, yield 73%). ^{1}H NMR (400 MHz, $CDCl_3$): δ (ppm) 7.75 (2H, d), 7.71 (2H, s), 7.68 (2H, d), 4.2 (8H, t), 2.10 (4H, m), 1.98 (4H, m), 1.09-0.94 (12H, m), 0.74 (6H, t), 0.53 (4H, m). Anal. calcd for $C_{31}H_{44}O_4B_2$: C, 74.13; H, 8.83; O, 12.74. Found: C, 74.04; H, 8.42; O, 12.63.

2.4 Polymerization

The polymerization was performed according to the general procedure of the Suzuki reaction[21]. A degassed mixture of toluene ([monomer] = 0.25M) and aqueous 2M potassium carbonate (3:2 in volume) was added into a mixture of 9,9-Dihexylfluorene-2,7-bis(trimethylene boronate), dibromo compound and tetrakis(triphenylp hosphine) palladium (1-2 mol %) in nitrogen atmosphere. The mixture was vigorously stirred at 85°C–90°C for 48 h, then cooled to room temperature. The mixture was poured into a mixture of methanol and deionized water (v:v = 10:1). The powdery polymer was obtained by filtration, and it was washed for 24 h in a Soxhlet apparatus with acetone to remove oligomers and catalyst residues. The resulting polymers were collected and dried under vacuum (yield: 50%–80%).

3 Results and Discussion

3.1 Synthesis and characterization

The general synthetic routes for the monomer synthesis and polymerization are as follows: 1,4-dialkylbenzene was synthesized from 1,4-dibromobenzene through the Grignard coupling reaction with alkylmagnesium bromide catalyzed by [1,3-bis(diphenylposphino)propane] (II) chloride. Dibromo compound was obtained by direct bromination of 9,9-dihexylfluorene and 1,4-dialkylbenzene with bromine and a small amount of ferric chloride as a catalyzing oxidizing reagent. 9,9-dihexylfluorene-2,7-bis(trimethylene boronate) was synthesized by using *n*-BuLi with a yield of 73%. The polymerization was based on the Suzuki coupling reaction, which was carried out in a mixture (3:2 in volume) of toluene and aqueous K_2CO_3 solution containing 1~2 mol % $Pd(PPh_3)_4$ under vigorous stirring at 85°C–90°C for 48 h in the nitrogen atmosphere. The chemical structures of the polymers obtained are shown in Scheme 1. All these polymers are air-stable and can be stored without any special precautions. They readily dissolve in common organic solvents, such as chloroform, THF, toluene and xylene. The chemical

structures of the polymers were verified by ^{1}H and

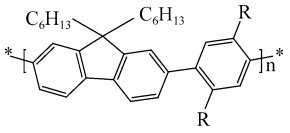

R= H PDHFP
R= C_6H_{13} PDHFDHP
R= C_8H_{17} PDHFDOP
R= $C_{10}H_{21}$ PDHFDDP

Scheme 1. Chemical structures of the polymers synthesized.

^{13}C NMR spectroscopy and elemental analysis. The number average molecular weights (*Mn*) of the polymers were determined by gel permeation chromatography (GPC) using polystyrene as the standard. The thermal stability of the polymers in nitrogen was evaluated by TGA. The corresponding data are summarized in Table 1. It can be seen that with increasing the length of alkyl side chain, the thermal decomposition temperature (T_d) of the substituted polymers increases first and then slightly decreases, compared with that of the unsubstituted polymer (PDHFP).

Table 1 Data of molecular weight, thermal analysis and optical properties

Polymer	M_n	M_w/M_n	T_g (℃)	T_d (℃)	λ_{max} (nm) (Solution)		λ_{max} (nm) (Film)	
					Abs.	Em.	Abs.	Em.
PDHFP	7 200	1.39	106.2	413	368	408 (432)	376	422 (442)
PDHFDHP	12 000	1.72	78.8	420	325	375	326	384
PDHFDOP	18 000	1.80	74.5	420	326	375	326	385
PDHFDDP	20 000	1.90	-	410	327	375	325	385

3.2 Optical properties

The spectroscopic properties of the polymers were measured in both solution ($CHCl_3$) and thin films, as shown in Fig. 1(a) and 1(b), respectively. And, the data on optical properties are summarized in Table 1. It can be seen that the peak of absorption spectra of the unsubstituted PDHFP in solution is at 368 nm while for the solid film, a red shift of the absorption was observed, and the absorption spectra in thin film is peaked at 376 nm. The red shift of the absorption spectra in thin film can be attributed to the intramolecular or intermolecular aggregation of the alternant copolymer in the solid state, which has been well documented for many other polymers[22, 23]. The substitution on the phenylene ring of PDHFP, however, induces an obvious substituent-dependent spectral change. The absorption peak of PDHFDHP is blue-shifted to 325 nm. This could be understood in terms of the steric hindrance of the hexyl chains, which decreases the coplanarity between the adjacent fluorene and phenylene units. When the substituent is changed (i.e. increased) from hexyl group (PDHFDHP) to decyl group (PDHFDDP), the absorption spectra of the polymers are close to those obtained from PDHFDHP. And all the substituted polymers show the absorption maxima at around 326 nm in both solution and the films. This suggests that there is no (or much less) aggregation formed in their solid films, which is due to the steric hindrance of the long alkyl chains at the phenylene units. However, the absorption spectra in solution exhibit a slight red shift with the increase of alkyl chain length on the phenylene ring, which probably indicates an increased entwisting tendency of longer alkyl side chains.

All the polymers emitted in blue to near-UV regions. The PL spectra of PDHFP were peaked at 408 nm in solution and 422 nm in the film. An obvious red shift (by 14 nm) was observed when changed from solution to film, probably due to the presence of aggregation formed in the film for the unsubstituted PDHFP. The emission peaks of all the other (substituted) polymers were located at 385 nm in the films. There is only a slight red shift with respect to their corresponding spectra in solution, probably indicating

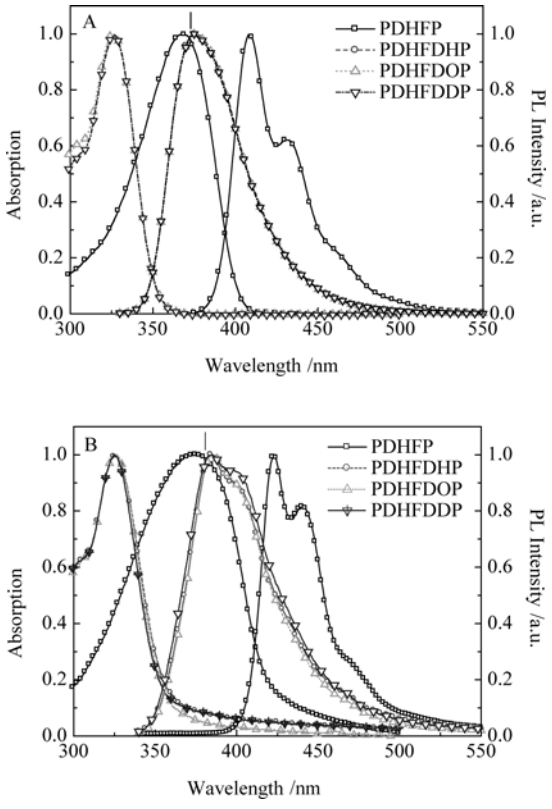

Fig. 1 UV-visible absorption spectra and photoluminescence (PL) spectra of polymers measured from (A) the chloroform solution (≈ 1×10^{-5} M) and (B) the spin-coated films on quartz plates at room temperature.

that there are no noticeable molecular conformation changes from solution to solid states because of the steric hindrance of the alkyl side groups.

In order to further investigate the effect of alkyl side chains on the optical properties, the polymer films were thermally treated in different manners and then their absorption and PL spectra were studied. Figure 2 shows the PL and absorption spectra of the polymer films annealed at different temperatures for different periods of time. When PDHFP film was annealed at 100°C, no spectral change was observed until annealing time was up to 1.5 h (Fig. 2(A)). When the annealing temperature was increased to 150℃ (for 3 h), however, an additional emission peak was clearly observed at around 515 nm in PL spectra for PDHFP. A broadening of the absorption spectra induced by annealing was observed. The appearance of the additional emission peak in PL spectra and the absorption spectra broadening for the unsubstituted PDHFP are attributed to the formation of excimer, as reported previously[24]. Similar annealing experiments were also applied to all the other substituted polymer films studied here. Compared with PDHFP, however, the spectral stability of the substituted polymer films was significantly improved because of the steric hindrance of the longer alkyl side chains, as shown in Fig. 2(B). Here, only the results for PDHFDHP were given as an example. The additional emission band (peak) observed at around 515 nm for PDHFP has been characterized as an unnoticeable shoulder for PDHFDHP. And it seems that the spectral stability does not exhibit noticeable dependence on the length of the alkyl chains for the substituted polymers.

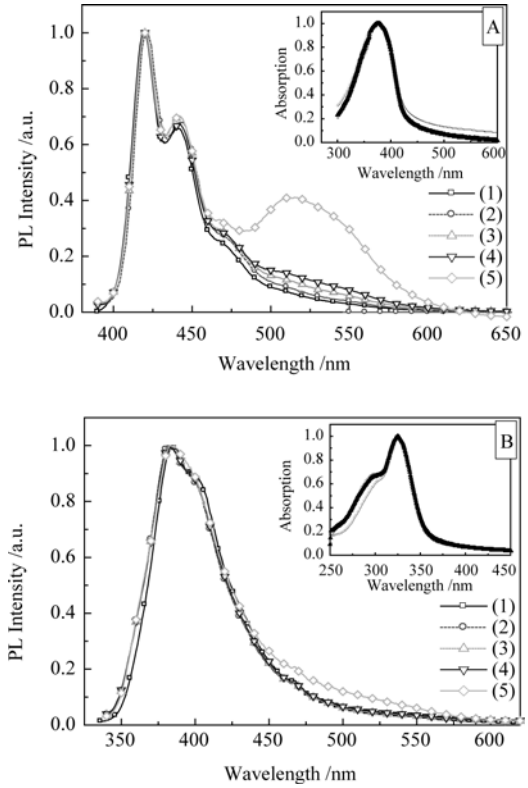

Fig. 2 Fluorescence spectra of PDHFP (A) and PDHFDHP (B): for the pristine film (1) and for the films annealed at 100°C for 30 min (2), 1.5 h (3), 3 h (4), and 150 °C for 3 h (5) in air. Inset: UV-vis absorption spectra of pristine (°C) and annealed films at 100 °C (○), 150 °C (Δ) for 3 h

In general, the fluorescent property of a conjugated polymer fundamentally depends on the nature of the conjugated backbone. However, the optical spectra of conjugated polymers are also heavily affected by the intramolecular or intermolecular interactions, which are dependent on film morphology and/or molecular chain packing. The absorption and PL spectra of PDHFP show an obvious red shift in the film compared with their corresponding spectra in solution. A pronounced emission peak appeared at 515 nm when PDHFP film was annealed at 150°C in air for 3 h. All these imply a strong intermolecular interaction and formation of aggregation excimer in PDHFP film. However, the UV absorption and PL spectra of PDHFDHP, PDHFDOP and PDHFDDP show no or slight red shift compared with their corresponding spectra in solution, and only a very weak emission band was observed at long wavelength region. It indicates that the substitution of alkyl side chains on the phenylene ring markedly decreases the formation tendency of aggregation excimer in solid films. This could be interpreted by a more effective separation of longer side chains to the molecular chains in all three dimensions, as demonstrated in other conjugated polymers[24].

3.3 Thermal behavior and liquid crystalline morphology

Most fluorene-based conjugated polymers exhibit interesting liquid crystalline features, which have been found to be potential applications in polarized light emission. Here, the thermal transition behavior and liquid crystalline textures were investigated as a function of side chain length by using DSC and microscopy techniques. Prior to the DSC scans, the powdery polymers were not thermally pretreated. DSC thermograms of the polymers are shown in Fig. 3 for the first heating scan. The glass transition

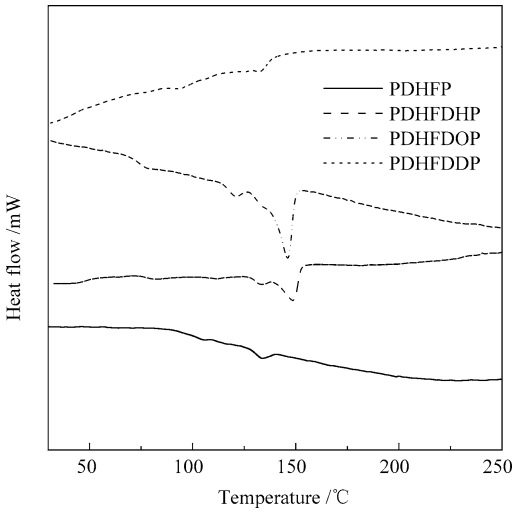

Fig. 3 DSC curves of the first heating run

temperature, T_g, is listed in Table 1. It can be seen that the values of T_g steadily decrease with the increase of the length of the alkyl side chain.

For the unsubstituted PDHFP, a weak step drop was observed at about 106.2°C in the first heating run, which was assigned as the glass transition. In addition, an endothermic peak was observed at around 133.8°C, which was attributed to the thermal transition ($T_{N\rightarrow I}$) from nematic phase to isotropic melt state (N → I). This phase transition was further demonstrated by a polarizing light microscopy (PLM) image shown in Fig.4 (a). The spin-cast pristine film of PDHFP is amorphous because of the absence of birefringence under PLM observation. However, the film annealed at 150°C displays a clear birefringence image (Fig. 4 (a)), indicating the existence of nematic liquid crystalline state. In the second heating run two endothermic peaks were observed at 105.4°C and 133.1℃, respectively, which were consistent with the first heating run. In the cooling run from the isotropic melt, PDHFP does not show any phase transition.

For PDHFDHP, the DSC thermogram of the first heating scan showed a glass transition at about 78.8°C (Fig. 3). Additionally, another two endothermic peaks at 133.6°C and 148.5°C were observed. In the second heating scan, however, in addition to an exothermic recrystallization peak at about 119.3°C two endothermic peaks were observed at 133.9°C and 148.5°C. Clearly, the first endothermic peak ($T_{C\rightarrow N}$) could be attributed to the phase transition from crystalline to nematic liquid crystalline state (C → N); and the second endothermic peak ($T_{N\rightarrow I}$) was due to the phase transition from nematic state to isotropic melt (N → I). No phase transition was observed in the cooling scan for PDHFDHP. Consistent with PDHFP, birefringence was not observed under PLM in the spin-cast pristine film of PDHFDHP, while a clear birefringence image (see Fig. 4(b)) appeared after annealing.

The difference of phase transition between PDHFP and PDHFDHP is evident. The DSC thermogram of the polymer (PDHFP) without alkyl side chains on the phenylene ring showed the glass transition and the nematic/isotropic phase transition. However, the DSC thermogram of the polymer (PDHFDHP) with substitutional alkyl side chains on the phenylene ring showed not only the glass transition and the nematic/isotropic phase transition, but also a recrystallization process and the crystalline/nematic phase transition. The DSC results suggest that the morphology of PDHFP is almost amorphous in solid state, and the morphology of the polymer with substitutional alkyl side chains on the phenylene ring is partially crystalline in solid state. The substitutional alkyls alter the intermolecular interaction and thus change the morphology of the polymers.

For PDHFDDP, two endothermic peaks were observed at 91.9°C and 131.7°C in the first heating run. In general, the glass transition temperature or softening point of conjugated backbone polymers decreases with the increase in the carbon number of alkyl side chains. It was reported that the softening point of polyfluorenes with alkyl substitution in C-9 site decreases from 94°C to 47°C, when the carbon number of alkyl chains increases from 6 to 12 [10]. Clearly, the first endothermic peak at 91.9°C could not be assigned as glass transition. Since the alkyl (here, decadal) side chain can partially form some ordered domains (i.e. the so-called side-chain crystallization), the first peak could thus be attributed to order-disorder transition of alkyl side chains

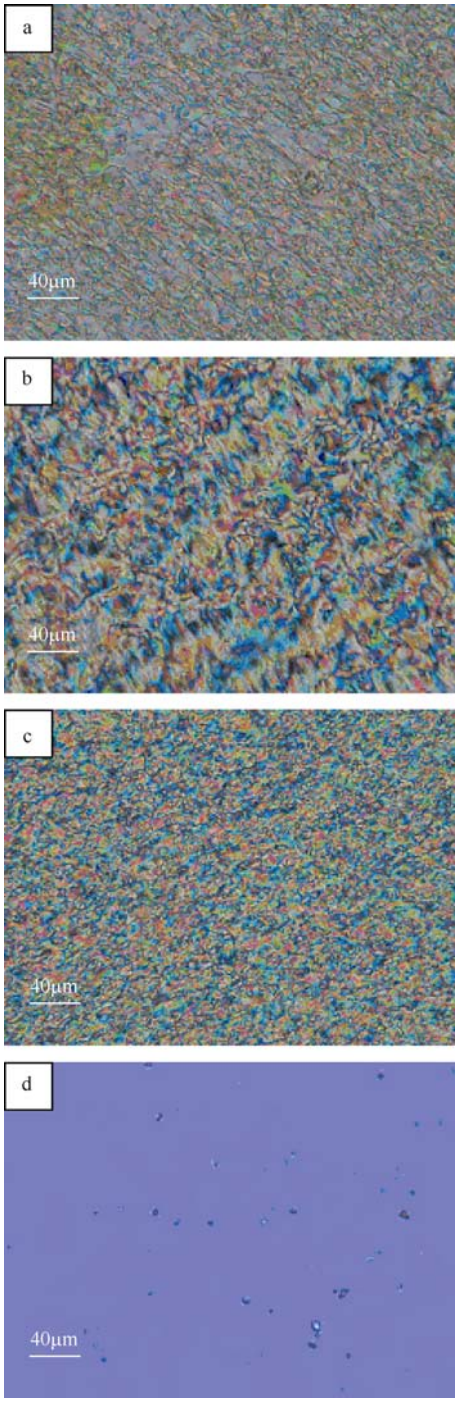

Fig. 4 Polarized light microscopy (PLM) images (× 500) of the films annealed at 150°C for PDHFP (**a**), PDHFDHP (**b**), PDHFDOP (**c**), and PDHFDDP (**d**)

during the heating process. In the second heating run, only one endothermic peak (at 132.6°C) was observed and the first peak observed in the first heating disappeared. The birefringence image was not observed under PLM in both pristine and annealed films of PDHFDDP (see Fig. 4(d)). No exothermal or endothermic peak was observed from the cooling run. The order-disorder transition of alkyl side chains has little effect on backbone arrangement or packing. The solid films are partially crystalline because of the substitution of alkyl side chains on the phenylene ring. Thus, the second peak at 131.7°C could be attributed to crystalline/isotropic melt phase transition.

For PDHFDOP, in addition to the presence of T_g (74.5°C) and T_m (146.1°C), an endothermic peak (121.2°C) and another unconspicuous endothermic peak (132.2°C) prior to the main melting peak were clearly observed in the thermogram of the first heating scan. However, in the second heating scan only an endothermic peak (134.6°C) was observed. The thermogram of the cooling scan did not show any exothermic or endothermic peak. The DSC results indicated that the phase transition process of PDFHDOP was similar to that of PDHFDHP and PDHFDDP. That is, the peak located at 121.2°C could be assigned to order-disorder transition of alkyl (octyl) groups, and the unconspicuous endothermic peak located at 132.2°C could be attributed to the crystalline/nematic liquid crystalline phase transition. The second heating scan thermogram of PDHFDOP implies that the enthalpy of phase transition from nematic liquid crystalline state to isotropic melt is too low to be detected by DSC. The pristine film did not display birefringence under PLM; after annealing at 150°C, the PLM image showed characteristic nematic liquid crystalline texture (see Fig. 4(c)).

The only structural difference among PDHFP, PDHFDHP, PDHFDOP and PDHFDDP is the length of the alkyl side chains. The DSC results suggest that the phase transition behavior of the polymers is clearly dependent on the length of alkyl side chains attached on the phenylene ring. The alkyl substitution on phenylene ring changes the intermolecular interaction. The increase of the side chains length will lead to stronger intermolecular interaction. The linear alkyl chains can partially form some ordered domains when the length of the side chains is long enough. Recent reports demonstrate that crystalline domains contributed little to the emission spectra [25, 26]. The substitution of alkyl chains restrains the formation of excimer due to steric hindrance and their efficient separation for backbones, and improves the thermal stability of spectra, compared with the unsubstituted PDHFP.

The self-assembled morphology of solvent-cast thin deposits of the polymers was investigated by TEM. In general, all the conjugated polymers studied here (i.e. so-called hairy-rod polymers) show a typical fibrillar morphology by self-assembly (Fig. 5), as observed in poly(3-alkylthiophenes)[27, 28], poly(9,9-dialkylfluorene) [29, 30] and poly(*para*-phenylene ethynylene)[31]. The molecular weight (*Mw*) of poly(3-hexylthiophene) [28] obviously dominates the morphology of the cast films. The well-defined nanorods formed in the low-*Mw* films are much larger than the ordered domains of the high-*Mw* films. In addition, the casting conditions or annealing treatment strongly affects the morphology of the low-*Mw* films, but has little effect on that of the high-*Mw* films. Near-field scanning microscopy studies on pristine films of poly(9,9-dialkylfluorene)[32, 33] have demonstrated the presence of fibrillar structures and show that the polymer chains are perpendicular to the ribbon axis. Here, the thermal treatment promotes the ordering degree of fibrillar structure (as indicated by a better phase contrast) (Fig. 5(b)), which is due to stronger intermolecular interaction and phase separation. Detailed studies about film morphology and molecular arrangement in these solid films affected by the change of side chain length in the polymers are under investigations in our lab.

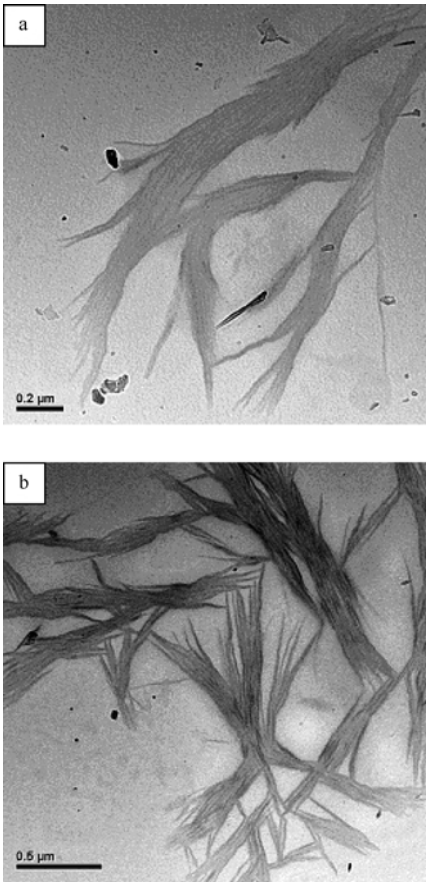

Fig. 5 TEM images of PDHFDHP: (**a**) pristine cast thin film, (**b**) annealed thin film at 80ºC for 30 min

4 Conclusions

A series of fluorene-*alt*-benzene based conjugated polymers with alkyl side chains of different lengths attached on phenylene ring were designed and synthesized. The polymers with alkyl side chains on phenylene ring induce

an obvious spectral blue shift, and the thermal spectral stability of the polymers is improved compared with that of the unsubstituted polymer. The alkyl substitutions alter the polymer intermolecular interaction and thus change the morphology of the polymers in solid state. The length of alkyl side chains attached on the phenylene ring also remarkably affected the thermal behavior (i.e. phase transition) of these polymers. The annealed films of the polymers display characteristic nematic liquid crystalline texture, and all polymers show the typical fibrillar morphology in solvent-cast thin deposits.

Acknowledgements This work was financially supported by the National Natural Science Foundation of China under Grant 50403012, the "Program for New Century Excellent Talents (NCET) in University"under Grant NCET-04-0355, and the "Shanghai Rising-Star Program" under Grant 04QMX1403.

6 References

1. Grell M., Bradley D. D. C., Inbasekaran M., Woo E. P., A glass-forming conjugated main-chain liquid crystal polymer for polarized electroluminescence applications, Adv. Mater. 1997, (9): 798
2. Scherf U., List E. J. W., Semiconducting polyfluorenes - Towards reliable structure-property relationships, Adv. Mater. 2002, (14): 477
3. He G. F., Li Y. F., Guo T. F., Yang Y., Thermal annealing induced high performance light-emitting diodes based on poly(9,9'-dioctyl fluorene), Synth. Met., 2003, (137): 1091–1092
4. Rughooputh S. D. D. V., Nowak M., Hotta S., Heeger A. J., Wudl F., Soluble conducting polymers - The poly(3-alkylthienylenes), Synth. Met., 1987, (21): 41–50
5. Leclene P., Hennebicq E., Calderone A., Brocorens P., Grimsdale A. C., Müllen K., Brédas J. L., Lazzaroni R., Supramolecular organization in block copolymers containing a conjugated segment: a joint AFM/molecular modeling study, Prog. Polym. Sci., 2003, (28): 55–81
6. Akcelrud L., Electroluminescent polymers, Prog. Polym. Sci., 2003, (28): 875–962
7. Geng Y. H., Culligan S. W., Trajkovska A., Wallace J. U., Chen S. H., Monodisperse oligofluorenes forming glassy-nematic films for polarized blue emission, Chem. Mater., 2003, (15): 542–549
8. Tirapattur S., Belletete M., Drolet N., Bouchard J., Ranger M., Leclerc M., Durocher G., Spectroscopic study of intermolecular interactions in various oligofluorenes: Precursors of light-emitting polymers, J. Phys. Chem. B, 2002, (106): 8959–8966
9. Nakazawa Y. K., Carter S. A., Nothofer H. G., Scherf U., Lee V. Y., Miller R. D., Scott J. C., Effects of polymer sidebranching in double- and single-layer polyfluorene light-emitting diodes, Appl. Phys. Lett., 2002, (80): 3832–3834
10. Teetsov J., Fox M. A., Photophysical characterization of dilute solutions and ordered thin films of alkyl-substituted polyfluorenes, J. Mater. Chem., 1999, (9): 2117–2122
11. Kawana S., Durrell M., Lu J., Macdonald J. E., Grell M., Bradley D. D. C., Jukes P. C., Jones R. A. L., Bennett S. L., X-ray diffraction study of the structure of thin polyfluorene films, Polymer, 2002, (43): 1907–1913
12. Tang H. Z., Fujiki M., Motonaga M., Alkyl side chain effects of optically active polyfluorenes on their chiroptical absorption and emission properties, Polymer, 2002, (43): 6213–6220
13. Tanto B., Guha S., Martin C. M., Scherf U., Winokur M. J., Structural and spectroscopic investigations of bulk poly [bis(2-ethyl)hexylfluorene], Macromolecules, 2004, (37): 9438–9448
14. Chen S. A., Ni J. M., Structure properties of conjugated conductive polymers. 1. Neutral poly(3-alkylthiophene)s, Macromolecules, 1992, (25): 6081–6089
15. Li Y. N., Vamvounis G., Holdcroft S., Tuning optical properties and enhancing solid-state emission of poly(thiophene)s by molecular control: a postfunctionalization approach, Macromolecules, 2002, (35): 6900–6906
16. Winokur M. J., Spiegel D., Kim Y., Hotta S., Heeger A. J., Structural and absorption studies of the thermochromic transition in poly(3-hexylthiophene), Synth. Met., 1989, (28): C419–C426
17. Redecker M., Bradley D. D. C., Inbasekaran M., Woo E. P., Mobility enhancement through homogeneous nematic alignment of a liquid-crystalline polyfluorene, Appl. Phys. Lett., 1999, (74): 1400–1402
18. Grell M., Bradley D. D. C., Inbasekaran M., Ungar G., Whitehead K. S., Woo E. P., Intrachain ordered polyfluorene, Synth. Met., 2000, (111): 579–581
19. Lieser G., Oda M., Miteva T., Meisel A., Nothofer H. G., Scherf U., Ordering, graphoepitaxial orientation, and conformation of a polyfluorene derivative of the "hairy-rod" type on an oriented substrate of polyimide, Macromolecules, 2000, (33): 4490–4495
20. Ranger M., Rondeau D., Leclerc M., New well-defined poly(2,7-fluorene) derivatives: Photoluminescence and base doping, Macromolecules, 1997, (30): 7686–7691
21. Liu B., Yu W. L., Lai Y. H., Huang W., Blue-light-emitting fluorene-based polymers with tunable electronic properties, Chem. Mater., 2001, (13): 1984–1991
22. Huang H. M., He Q. G., Song Y., Lin H. Z., Yang J. L., Bai F. L., Synthesis and photophysical properties of alternating copolymers containing triphenylamine moieties, Polym. Adv. Technol., 2003, (14): 309–313
23. Lemmer U., Heun S., Mahrt R. F., Scherf U., Hopmeier M., Siegner U., Göbel E. O., Müllen K., Bässler H., Aggregate fluorescence in conjugated polymers, Chem. Phys. Lett., 1995, (240): 373–378
24. Zeng G., Yu W. L., Chua S. J., Huang W., Spectral and thermal spectral stability study for fluorene-based conjugated polymers, Macromolecules, 2002, (35): 6907–6914
25. Chen S. H., Su A. C., Chang C. S., Chen H. L., Ho D. L., Tsao C. S., Peng K. Y., Chen S. A., Aging of poly(2-methoxy-5-(2'-ethylhexyloxy)-1,4-phenylenevinylene)/toluene solutions and subsequent effects on luminescence behavior of cast films, Langmuir, 2004, (20): 8909–8915
26. Chen S. H., Su A. C., Su C. H., Chen S. A., Crystalline forms and emission behavior of poly(9,9-di-n-octyl-2,7-fluorene), Macromolecules, 2005, (38): 379–385
27. Ihn K. J., Moulton J., Smith P., Whiskers of poly(3-alkylthiophene)s, J. Polym. Sci. Part B: Polym. Phys., 1993, (31): 735–742
28. Kline R. J., McGehee M. D., Kadnikova E. N., Liu J. S., Fréchet J. M. J., Toney M. F., Dependence of regioregular poly(3-hexylthiophene) film morphology and field-effect mobility on molecular weight, Macromolecules, 2005, (38): 3312–3319
29. Surin M., Hennebicq E., Ego C., Marsitzky D., Grimsdale A. C., Müllen K., Brédas J. L., Lazzaroni R., Leclère P., Correlation between the microscopic morphology and the solid-state photoluminescence properties in fluorene-based polymers and copolymers, Chem. Mater., 2004, (16): 994–1001
30. Chappell J., Lidzey D. G., Jukes P. C., Higgins A. M., Thompson R. L., O'Connor S., Grizzi I., Fletcher R., O'Brien J., Geoghegan M., Jones R. A. L., Correlating structure with

fluorescence emission in phase-separated conjugated-polymer blends, Nature Mater., 2003, (2): 616–621
31. Samorì P., Sikharulidze I., Francke V., Müllen K., Rabe J. P., Nanoribbons from conjugated macromolecules on amorphous substrates observed by SFM and TEM, Nanotechnology, 1999, (10): 77–80
32. Teetsov J. A., Vanden Bout D. A., Imaging molecular and nanoscale order in conjugated polymer thin films with near-field scanning optical microscopy, J. Am. Chem. Soc., 2001, (123): 3605–3606
33. Teetsov J., Vanden Bout D. A., Near-field scanning optical microscopy studies of nanoscale order in thermally annealed films of poly(9,9-diakylfluorene), Langmuir, 2002, (18): 897–903